THE JOURNAL OF BIOLOGICAL CHEMISTRY VOL. 289, NO. 14, pp. 10168–10181, April 4, 2014


# Characterization of *Schizosaccharomyces pombe* Copper Transporter Proteins in Meiotic and Sporulating Cells*

Received for publication, December 16, 2013, and in revised form, February 20, 2014 Published, JBC Papers in Press, February 25, 2014, DOI 10.1074/jbc.M113.543678

**Samuel Plante**[1], **Raphaël Ioannoni**[2], **Jude Beaudoin, and Simon Labbé**[3]

*From the Département de Biochimie, Faculté de Médecine et des Sciences de la Santé, Université de Sherbrooke, Sherbrooke, Quebec J1E 4K8, Canada*

**Background:** Despite a requirement for copper during meiosis, the role of copper transporters (Ctrs) in this process remains poorly understood.
**Results:** Ctrs exhibit temporal and dynamic cellular localization patterns during meiotic differentiation.
**Conclusion:** Whereas Ctr4/5 is primarily involved during early meiosis, Ctr6 is present throughout the entire program and is associated with a non-canonical cellular location.
**Significance:** A dynamic interplay between copper transport systems occurs during meiosis.

**Meiosis requires copper to undertake its program in which haploid gametes are produced from diploid precursor cells. In *Schizosaccharomyces pombe*, copper is transported by three members of the copper transporter (Ctr) family, namely Ctr4, Ctr5, and Ctr6. Although central for sexual differentiation, very little is known about the expression profile, cellular localization, and physiological contribution of the Ctr proteins during meiosis. Analysis of gene expression of *ctr4*$^+$ and *ctr5*$^+$ revealed that they are primarily expressed in early meiosis under low copper conditions. In the case of *ctr6*$^+$, its expression is broader, being detected throughout the entire meiotic process with an increase during middle- and late-phase meiosis. Whereas the expression of *ctr4*$^+$ and *ctr5*$^+$ is exclusively dependent on the presence of Cuf1, *ctr6*$^+$ gene expression relies on two distinct regulators, Cuf1 and Mei4. Ctr4 and Ctr5 proteins co-localize at the plasma membrane shortly after meiotic induction, whereas Ctr6 is located on the membrane of vacuoles. After meiotic divisions, Ctr4 and Ctr5 disappear from the cell surface, whereas Ctr6 undergoes an intracellular re-location to co-localize with the forespore membrane. Under copper-limiting conditions, disruption of *ctr4*$^+$ and *ctr6*$^+$ results in altered SOD1 activity, whereas these mutant cells exhibit substantially decreased levels of CAO activity mostly in early- and middle-phase meiosis. Collectively, these results emphasize the notion that Ctr proteins exhibit differential expression, localization, and contribution in delivering copper to SOD1 and Cao1 proteins during meiosis.**

Copper transport is essential for a number of biological processes, including respiration, antioxidant defense, xenobiotic amine metabolism, and meiosis (1, 2). Because of its property to lose and accept one electron, copper is not only required as a catalytic cofactor, but it can also participate in Fenton-like reactions that generate the highly toxic hydroxyl radical that may cause cellular damage (3). To balance the need for copper while at the same time preventing its accumulation to cytotoxic levels, organisms have developed mechanisms to control their internal copper load, including the use of specialized copper transporters.

In *Schizosaccharomyces pombe*, three proteins are members of the copper transporter (Ctr)[4] family (4). Two of these, Ctr4 and Ctr5, form a heteroprotein complex at the plasma membrane of cells that grow mitotically (vegetative growth) under low copper conditions. Ctr4 and Ctr5 are interdependent for maturation through the secretory pathway and for copper transport activity when present at the cell surface (5). As is the case for most members of the Ctr family, Ctr4 and Ctr5 harbor extracellular N-terminal hydrophilic regions that contain methionine residues organized as $MX_2M$ and/or $MXM$ motifs (denoted Mets motifs) (6). The primary structure of Ctr4 and Ctr5 also contains three transmembrane domains (TMDs), a $MX_3M$ motif within their second TMD and a $GX_3G$ motif within their third TMD. The last two motifs are predicted to play key roles in copper uptake and assembly of Ctr4-Ctr5 as a heterotrimeric complex, respectively (7–9). Bimolecular fluorescence complementation experiments have shown that the assembly of a functional heterotrimeric Ctr4-Ctr5 complex at the cell surface requires a combination of two Ctr4 molecules with one Ctr5 molecule (10). As expected, cells containing a deletion of *ctr4*$^+$ or *ctr5*$^+$ gene exhibit copper starvation phenotypes characterized by their inability to take up $^{64}Cu$ and show poor cell growth on low copper medium and alterations in copper-dependent enzymes activity (*e.g.* SOD1, copper amine oxidase 1 (Cao1) and cytochrome *c* oxidase) (5, 11, 12).

A third member of the Ctr family, denoted Ctr6, localizes on the membrane of vacuoles in cells proliferating in mitosis under

* This work was supported by Canadian Institutes of Health Research Grant MOP-CP-243929 (to S. L.).
[1] Recipient of a studentship from the Foundation of Stars for Children's Health Research.
[2] Recipient of a studentship from the Natural Sciences and Engineering Research Council of Canada.
[3] To whom correspondence should be addressed: Faculté de Médecine et des Sciences de la Santé, 3201, Pavillon Z-8, Jean Mignault, Sherbrooke, QC, J1E 4K8, Canada. Tel.: 819-821-8000 (ext. 75460); Fax: 819-820-6831; E-mail: Simon.Labbe@USherbrooke.ca.

[4] The abbreviations used are: Ctr, copper transporter; BCS, bathocuproinedisulfonic acid; Cao1, copper amine oxidase 1; CAO, copper amine oxidase; Cherry, red fluorescent protein; Cuf1, copper factor 1; EMM, Edinburgh minimal medium; Mfc1, major facilitator copper transporter 1; TTM, ammonium tetrathiomolybdate; TMD, transmembrane domain.

low copper conditions (13). The N-terminal region of Ctr6 contains a M*X*HCXMXM motif that is involved in the process of copper transport. The predicted topology of Ctr6 suggests that the protein possesses three TMDs and conserved motifs found in the Ctr family of copper transporters, including a $MX_3M$ motif in TMD2 and a $GX_3G$ motif in TMD3 that may be responsible for the assembly of Ctr6 as a homotrimer. The use of mutant strains has revealed that the inactivation of *ctr6*$^+$ (*ctr6*Δ) within the context of a *ctr4*Δ mutant strain results in a complete loss of SOD1 activity, revealing a function for Ctr6 in providing copper to at least one cytosolic copper-dependent enzyme under low copper conditions (13). On the basis of studies on Ctr6 and its ortholog Ctr2 in *S. cerevisiae* (14, 15), a current model suggests that Ctr6 mediates the efflux of copper from the vacuole into the cytosol when cells undergo a transition from copper-sufficient to copper-limiting conditions.

Meiosis is a specialized mode of cell division by which precursor diploid cells produce haploid gametes (16, 17). To achieve this, diploid cells replicate their chromosomal DNA, generating pairs of homologous chromosomes that are subsequently subjected to homologous recombination. Following this process, homologous chromosomes and sister chromatids are successively separated during the first (MI) and second (MII) meiotic divisions, respectively. Once MI and MII divisions are completed, a differentiation phase occurs in order to produce four mature gametes that are competent for fertilization or germination. Studies in yeast and mice have shown that metal ions such as zinc and copper are essential for normal progression of meiosis (18–20). Insufficient concentrations of these metal ions lead to meiotic arrests as well as errors during meiosis. Despite the known essential role for copper during meiotic differentiation, copper requirement and copper transport proteins involved in this developmental process remain poorly understood.

*S. pombe* is a genetically amenable organism that is commonly used for identifying and characterizing cellular components that regulate molecular aspects of meiosis (21). This yeast is of special interest as growth conditions and temperature-sensitive mutants have been developed that allow synchronization of cells for their entry into the meiotic program (22, 23). Under conditions of nitrogen starvation, haploid cells arrest in the $G_1$ phase of the cell cycle. If cells of the opposite mating type are found together under these conditions, haploid cells conjugate to form diploid cells, and the resulting zygotes usually undergo meiosis by a process called zygotic meiosis. If the resulting zygotes are transferred to a nitrogen-rich medium immediately after conjugation, cells can grow as diploids for a period of time. Over this period of time, if these diploid cells undergo a second transition from high to low nitrogen, their commitment to meiosis occurs quickly and in a more efficacious and synchronous manner in comparison with zygotic meiosis. This process is called azygotic meiosis. During the mitotic cell cycle cells express the Pat1 kinase that inhibits the initiation of meiosis by phosphorylating the meiotic transcription factor Ste11 and the meiosis-specific inducer Mei2 (21). A mutant strain carrying a temperature-sensitive *pat1-114* allele produces a thermolabile Pat1 kinase. After a heat shock at 34 °C, Pat1 is readily inactivated, fostering the cell cycle switch from mitosis to meiosis in a highly efficient and synchronous manner. This latter system called *pat1*-induced meiosis is more synchronous than azygotic meiosis. Initiation as well as progression and conclusion of meiosis involve four successive waves of gene expression that are mainly controlled by meiosis-specific transcription factors (24, 25). A first wave of expressed genes includes those that are induced by nitrogen starvation and pheromones. Several of these genes are under the control of Ste11 and are primarily involved in initiating meiosis. Subsequently, a second wave of genes (denoted early genes) is activated by Rep1. Products of these genes are involved in premeiotic DNA replication and recombination. After this stage, Mei4 activates expression of middle meiotic genes (third wave) whose products are involved in meiotic divisions and early steps of spore formation. The expression of many several middle genes is subsequently repressed by the transcription factor Cuf2 (26). Late gene expression (fourth wave) is controlled by several transcription factors, including Rev2, Atf21, and Atf31. The products of these genes are required for spore maturation.

Investigation of copper starvation response during meiosis has revealed that the expression of *ctr4*$^+$ is induced after 30 min of meiotic induction followed by its repression 3 h after entry into meiosis (19). Consistent with meiotic *ctr4*$^+$ transcript levels, a functional GFP epitope-tagged Ctr4 protein is detected at the cell surface of zygotic cells within the first hour of meiosis and remains there until the 3-h meiotic time point is reached and then it disappears from the cell surface (19). At that stage, a meiosis-specific gene, *mfc1*$^+$, is induced in response to copper starvation and remains expressed throughout the meiotic program (19). *mfc1*$^+$ encodes a putative major facilitator superfamily-type transporter. At the 3-h meiotic time point, a functional Cherry epitope-tagged Mfc1 protein is first observed on membranes of small intracellular vesicles. At the 6-h meiotic time point, Mfc1-Cherry-associated fluorescence localizes at the forespore membrane where it plays an important role for copper accumulation into forespores and the production of fully active Cao1 (copper amine oxidase 1), which localized primarily in the forespores of asci (19).

In the present study proteins involved in copper transport during meiosis and the profiles of expression of *ctr5*$^+$ and *ctr6*$^+$ were determined and compared with that of *ctr4*$^+$. Although Cuf1 was required for expression of *ctr4*$^+$ and *ctr5*$^+$ during meiosis, *ctr6*$^+$ expression required the presence of Mei4 in addition to Cuf1. As opposed to *ctr4*$^+$ and *ctr5*$^+$ that are primarily expressed under low copper conditions, *ctr6*$^+$ mRNA levels were detected in meiotic cells under standard, copper-depleted, and copper-replete conditions. Consistent with their gene expression profiles, Ctr4 and Ctr5 proteins co-localized at the plasma membrane shortly after induction of meiosis and then progressively disappeared after 3 h of meiotic induction. In the case of Ctr6, the protein localized to vacuolar membranes in early meiosis and then underwent redistribution in a time-dependent manner to reach forespore membranes where it persisted until sporulation. Under copper starvation conditions, meiotic *ctr4*Δ *ctr6*Δ cells were defective in SOD1 activity. Although these cells (*ctr4*Δ *ctr6*Δ) exhibited a lower level of CAO activity in early meiosis, their CAO activity significantly increased after 6 h of meiotic induction. The increase of CAO

activity was due to the presence of Mfc1, as a triple mutant *ctr4*Δ *ctr6*Δ *mfc1*Δ strain was unable to exhibit an increase of CAO activity (6 h after induction of meiosis). Together the results revealed that during the meiotic program, copper transporters are expressed and localized in a time-dependent manner, exhibiting distinct contributions in delivering copper to two meiotic copper-dependent enzymes, SOD1 and Cao1.

## EXPERIMENTAL PROCEDURES

*Strains and Media*—*S. pombe* strains used in this study are listed in Table 1. Standard methods were used for growth, mating, and sporulation of cells (27). Under nonselective conditions, cells were grown on yeast extract plus supplements containing 0.5% yeast extract, 2% glucose, and 225 mg/liter adenine, histidine, leucine, uracil, and lysine. To integrate or transform plasmids into strains, Edinburgh minimal medium (EMM) supplemented with 225 mg/liter of the required amino acids was used. Unsupplemented EMM medium contained 160 nM copper. The $h^+/h^-$ diploid strains used for azygotic meiosis were isolated as described previously (26), and the resulting zygotes were returned to rich medium (yeast extract plus supplements) before commitment to meiosis. Diploid cells underwent azygotic meiosis after a synchronized nitrogen-starvation shock in which EMM lacking nitrogen was supplemented with 10 mg/liter of adenine or 10 mg/liter of adenine, histidine, leucine, uracil, and lysine. Diploid strains homozygous for the mating type ($h^+/h^+$) were generated by incubating mid-logarithmic cultures of haploid cells with 20 μg/ml carbendazim (Sigma) as described previously (28). To synchronize *pat1-114*$^{ts}$ diploid cells for their entry into meiosis, they were precultured in EMM supplemented with adenine (225 mg/liter) at 25 °C for 48 h. At mid-logarithmic phase (cell titer of $\sim 1 \times 10^7$ cells/ml), cells were harvested, washed twice, and transferred to EMM lacking nitrogen supplemented with 10 mg/liter of adenine. After incubation for 16 h at 25 °C, $NH_4Cl$ (5 mg/liter) was added to the culture medium, and cells were split and treated with either ammonium tetrathiomolybdate (TTM) (Sigma) or $CuSO_4$ or were left untreated. At this point the temperature was rapidly raised (to 34 °C) to induce meiosis, as described previously (19). Meiosis progression of zygotes was monitored by adding 5 μg/ml Hoechst 33342 stain (Invitrogen) at different times after meiotic induction at 34 °C.

*Plasmids*—To create a plasmid that possessed the *ctr6*$^+$ promoter driving expression of the *ctr6*$^+$-*HA*$_4$ fusion allele, the *ctr6*$^+$ 5′ regulatory region (positions −650 to −1) was amplified by PCR and inserted immediately upstream of the ATG codon of the *ctr6*$^+$-*HA*$_4$ gene into the ApaI/XhoI-digested p*ctr6*$^+$-*HA*$_4$ plasmid (13). Subsequently, the ApaI-BamHI DNA fragment containing the *ctr6*$^+$ promoter and the coding region of *ctr6*$^+$-*HA*$_4$ was cloned into the corresponding sites of pJK148 (29). The integrative plasmid pJK*ctr4*$^+$-*GFP* was generated by subcloning the PstI-SpeI fragment from pBP*ctr4*$^+$-*GFP* (6) containing the entire *ctr4*$^+$-*GFP* fusion gene under the control of its own promoter (positions −737 to −1) into the corresponding sites of pJK148. To create pJK*prom-ctr5*$^+$, a PstI-XmaI PCR-amplified fragment containing the *ctr5*$^+$ gene along with its promoter (up to −815 from the initiator codon) was cloned into pJK210 (29). The *Cherry* coding sequence derived from BM46*SITmCherry* (30) was isolated by PCR using primers designed to produce XmaI and SacI sites at the 5′ and 3′ termini of the *Cherry* gene. The resulting DNA fragment was used to clone the *Cherry* coding sequence into pJK*prom-ctr5*$^+$ plasmid to which XmaI and SacI restriction sites had previously been

**TABLE 1**
***S. pombe* strain genotypes**

| Strain | Genotype | Source or Reference |
|---|---|---|
| FY435 | *h*$^+$ *his7-366 leu1-32 ura4-Δ18 ade6-M210* | 19 |
| FY436 | *h*$^-$ *his7-366 leu1-32 ura4-Δ18 ade6-M216* | 19 |
| DBY6 | *h*$^+$ *his7-366 leu1-32 ura4-Δ18 ade6-M210 ctr6Δ::hisG* | 13 |
| SPY1 | *h- his7-366 leu1-32 ura4-Δ18 ade6-M216 ctr6Δ::LoxP* | This study |
| DBY11 | *h*$^+$ *his7-366 leu1-32 ura4-Δ18 ade6-M210 ctr6Δ::hisG ctr4Δ::URA4* | 13 |
| SPY2 | *h*$^-$ *his7-366 leu1-32 ura4-Δ18 ade6-M216 ctr6Δ::LoxP ctr4Δ::LoxPKANr* | This study |
| SPY3 | *h*$^+$ *his7-366 leu1-32 ura4-Δ18 ade6-M210 ctr4Δ::LoxP ctr5Δ::KANr* | This study |
| SPY4 | *h*$^-$ *his7-366 leu1-32 ura4-Δ18 ade6-M216 ctr4Δ::LoxP ctr5Δ::KANr* | This study |
| JSY104 | *h*$^+$ *his7-366 leu1-32 ura4-Δ18 ade6-M210 ctr4Δ::KAN*$^r$ | 19 |
| JSY204 | *h*$^-$ *his7-366 leu1-32 ura4-Δ18 ade6-M216 ctr4Δ::KAN*$^r$ | 19 |
| SPY5 | *h*$^+$ *his7-366 leu1-32 ura4-Δ18 ade6-M210 mfc1Δ::LoxP ctr4Δ::LoxP ctr6Δ::KANr* | This study |
| SPY6 | *h*$^-$ *his7-366 leu1-32 ura4-Δ18 ade6-M210 mfc1Δ::LoxP ctr4Δ::LoxP ctr6Δ::KANr* | This study |
| FY435/FY436 | *h+/h- his7-366/his7-366 leu1-32/leu1-32 ura4Δ18/ura4Δ18 ade6-M210/ade6-M216* | This study |
| ctr6Δ/Δ | *h+/h- his7-366/his7-366 leu1-32/leu1-32 ura4Δ18/ura4Δ18 ade6-M210/ade6-M216 ctr6Δ::HisG/ctr6Δ::LoxP* | This study |
| ctr4Δ/Δ | *h+/h- his7-366/his7-366 leu1-32/leu1-32 ura4Δ18/ura4Δ18 ade6-M210/ade6-M216 ctr4Δ::KAN/ctr4Δ::KAN* | This study |
| ctr4Δ/Δ/ctr6Δ/Δ | *h+/h- his7-366/his7-366 leu1-32/leu1-32 ura4Δ18/ura4Δ18 ade6-M210/ade6-M216 ctr6Δ::HisG/ctr6Δ::LoxP ctr4Δ::KAN/ctr4Δ::KAN* | This study |
| mfc1Δ/Δ/ctr6Δ/Δ/ ctr4Δ/Δ | *h+/h- his7-366/his7-366 leu1-32/leu1-32 ura4Δ18/ura4Δ18 ade6-M210/ade6-M216 mfc1Δ::LoxP/mfc1Δ::LoxP ctr4Δ::LoxP/ctr4Δ::LoxP ctr6Δ::KAN/ctr6Δ::KAN* | This study |
| JSY5 | *h*$^+$ *pat1-114 ade6-M210 ctr4Δ::KAN*$^r$ | 19 |
| JSY6 | *h*$^+$ *pat1-114 ade6-M216 ctr4Δ::KAN*$^r$ | 19 |
| JB484 | *h*$^+$ *pat1-114 ade6-M210* | 22 |
| JB485 | *h*$^+$ *pat1-114 ade6-M216* | 22 |
| RAY14 | *h*$^+$ *pat1-114 ade6-M210 mei4Δ::KAN*$^r$ | 26 |
| RAY15 | *h*$^+$ *pat1-114 ade6-M216 mei4Δ::KAN*$^r$ | 26 |
| JSY3 | *h*$^+$ *pat1-114 ade6-M210 cuf1Δ::KAN*$^r$ | 19 |
| JSY4 | *h*$^+$ *pat1-114 ade6-M216 cuf1Δ::KAN*$^r$ | 19 |
| SPY7 | *h*$^+$ *pat1-114 ade6-M210 mei4Δ::loxP cuf1Δ::KAN*$^r$ | This study |
| SPY8 | *h*$^+$ *pat1-114 ade6-M216 mei4Δ::loxP cuf1Δ::KAN*$^r$ | This study |

introduced by PCR and placed immediately upstream of the *ctr5*$^+$ stop codon. For this construct, denoted pJK*ctr5*$^+$*-Cherry*, the XmaI-SacI *Cherry*-encoded fragment was inserted in-frame with the C-terminal region of Ctr5. The *cao1*$^+$*-GFP* fusion gene with its own promoter and terminator was isolated from the pSP1*cao1*$^+$*-GFP* plasmid (12) using SpeI and ApaI. Once purified, the DNA fragment was inserted into the corresponding restriction sites of pJK148, generating pJK*cao1*$^+$*-GFP*. *ctr6*$^+$*-lacZ* fusion plasmids were created using similar DNA molecular cloning approaches as described previously (13).

*RNA Isolation and Analysis*—Total RNA was extracted by a hot phenol method as described previously (31). RNA samples were quantified by spectrophotometry, and 15 $\mu$g of RNA per sample were used for the RNase protection assays, which were performed as described previously (32). To detect *ctr6*$^+$ mRNA levels, plasmid pSK*ctr6*$^+$-v2 was generated by inserting a 198-bp BamHI-EcoRI fragment from the *ctr6*$^+$ gene into the same restriction sites of pBluescript SK (Stratagene, La Jolla, CA). The antisense RNA hybridizes to the region between positions +95 and +293 downstream of the first base of the translational start codon of *ctr6*$^+$. To create pSK*ctr5*$^+$-v1, a 187-bp fragment from the *ctr5*$^+$ gene (corresponding to the coding region between positions +301 and +482) was amplified and cloned into the BamHI-EcoRI sites of pBluescript SK. Plasmids pSK*ctr4*$^+$ (33), pSK*cuf1*$^+$-v7 (19), pSK*mei4*$^+$ (26), pKS*lacZ*, and pSK*act1*$^+$ (34) were used to produce antisense RNA probes, allowing the detection of steady-state levels of *ctr4*$^+$, *cuf1*$^+$, *mei4*$^+$, *lacZ*, and *act1*$^+$ mRNAs, respectively. $^{32}$P-Labeled antisense RNA probes were produced from the above-mentioned BamHI-linearized plasmids and with the use of [$\alpha$-$^{32}$P]UTP and the T7 RNA polymerase. The *act1*$^+$ riboprobe was used to detect *act1*$^+$ mRNA as an internal control for normalization during quantification of the RNase protection products.

*Direct and Indirect Immunofluorescence Microscopy*—Diploid *h*$^+$/*h*$^-$ *ctr4*Δ/*ctr4*Δ *ctr5*Δ/*ctr5*Δ cells co-expressing *ctr4*$^+$*-GFP*/*ctr4*$^+$*-GFP* and *ctr5*$^+$*-Cherry*/*ctr5*$^+$*-Cherry* were synchronously induced to enter in azygotic meiosis. At zero time point, when cells had just entered meiosis and for the subsequent time points, culture aliquots were retrieved every hour. At each time point, Hoechst 33342 stain (5 $\mu$g/ml) was added to analyze progression of meiosis of individual cells. At the indicated times, cells were subjected to microscopic analysis using a 1000× magnification and the following filters: 340–380 nm (Hoechst 33342), 465–495 nm (GFP), and 510–560 nm (Cherry). For localization of Ctr6 in mitotically growing cells, *ctr6*Δ mutant cells were transformed with the integrative plasmid p*ctr6*$^+$*-HA*$_4$, which expresses a functional *HA*$_4$ epitope-tagged Ctr6 protein (13). Indirect immunofluorescence microscopy was performed as described previously (6, 13), except that cells were fixed with formaldehyde (methanol-free) after a 3-h incubation in the presence of bathocuproinedisulfonic acid (BCS). In the case of Ctr6-*HA*$_4$ localization during the meiotic program, *h*$^+$/*h*$^-$ *ctr6*Δ/*ctr6*Δ diploid cells expressing *ctr6*$^+$*-HA*$_4$/*ctr6*$^+$*-HA*$_4$ were induced in azygotic meiosis and separated into different lots that were left untreated or treated with TTM and $CuSO_4$. At the indicated meiotic phase, cells were fixed and adsorbed on poly-L-lysine-coated (0.1%) multiwall slides as described previously (13). After a 30-min block with TNB (10 mM Tris/HCl, pH 7.5, 150 mM NaCl, 1% BSA, 0.02% sodium azide), cells were incubated with anti-HA antibody (F-7) (Santa Cruz Biotechnology, Santa Cruz, CA) diluted 1:250 in TNB. After an 18-h incubation at 4 °C, cells were washed with TNB and incubated for 4 h with a goat anti-mouse Alexa Fluor 546-labeled IgG antibody (Invitrogen) diluted 1:250 in TNB. After cells were washed, mounting media (Invitrogen) containing Hoechst 33342 stain was added to each well unless otherwise stated. Vacuole membrane staining using FM4–64 (Sigma) was performed as described previously (35). Briefly, mid-logarithmic copper-starved cells were harvested and resuspended in yeast extract plus supplements medium containing BCS (100 $\mu$M) and FM4–64 (16 $\mu$M) for 30 min at 30 °C. Cells were pelleted, washed, resuspended in fresh BCS-containing yeast extract plus supplements and incubated at 30 °C for an additional 30 min. Fluorescence and differential interference contrast images of the cells were obtained using a Nikon Eclipse E800 epifluorescent microscope (Nikon, Melville, NY) equipped with a Hamamatsu ORCA-ER digital cooled charge-coupled device (CCD) camera (Hamamatsu, Bridgewater, NJ). Fields shown in this study are representative of at least five independent experiments. Merged images were obtained using the Simple PCI software version 5.3.0.1102 (Compix, Sewickly, PA).

*SOD and CAO Activity Assays*—Protein extracts were prepared from mid-logarithmic cells that had been incubated for 16 h with either BCS (100 $\mu$M) or $CuSO_4$ (50 $\mu$M) unless otherwise stated. After treatments, cells were harvested and washed with lysis buffer containing 25 mM Tris-HCl, pH 7.5, 150 mM NaCl, 1 mM PMSF, 1 mM DTT, 0.1 mM $Na_3VO_4$, and a protease inhibitor mixture (Sigma; P8340). Once washed, cells were suspended in 200 $\mu$l of lysis buffer and then disrupted with an equivalent volume of glass beads using a Fastprep instrument (MP Biomedicals). Lysates were centrifuged at 13,000 × *g* for 15 min at 4 °C, and then the supernatants that contained soluble proteins were partially purified using Spin-X centrifuge tube filters (Costar-Corning; 8161). Equal concentrations of lysates were analyzed on 10% native polyacrylamide gels as described previously (36), and SOD activity assays were carried out using in-gel nitro blue tetrazolium staining as described previously (11). Spectrophotometric determination of SOD activity was performed using a cytochrome *c*/xanthine oxidase method (13). CAO activity was determined by spectrophotometry as described previously (12). In these assays hydrogen peroxide that is released is quantitated using 4-aminoantipyrine and vanillic acid to generate a quinoneimine dye, which is detected at 498 nm.

*Immunoblotting and ChIP*—For Western blotting experiments, protein extracts were resolved on 12% or 15% sodium dodecyl sulfate-polyacrylamide gels. For protein expression analysis of SOD1, Cao1, and $\alpha$-tubulin, the following primary antibodies were used for immunodetection: monoclonal anti-SOD1 antibody (SOD-100; Stressgen), monoclonal anti-His$_5$ antibody (penta-His; Qiagen), and monoclonal anti-$\alpha$-tubulin antibody (clone B-5–1-2; Sigma), respectively. After incubation with primary antibodies, membranes were washed and incubated with the appropriate horseradish peroxidase-conjugated secondary antibodies (Amersham Biosciences), developed with ECL reagents (Amersham Biosciences), and visualized by chemiluminescence. Cao1 was detected by immunoblotting

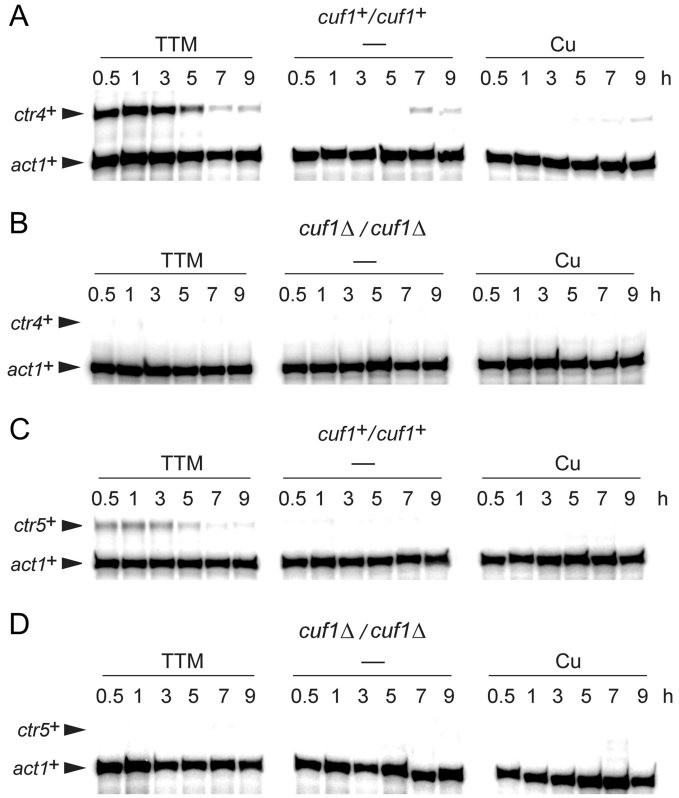


FIGURE 1. **The cuf1$^+$ gene is required for copper starvation-dependent induction of ctr4$^+$ and ctr5$^+$ transcripts during meiosis.** Representative expression profiles of *ctr4*$^+$ and *ctr5*$^+$ transcripts in *pat1-114/pat1-114 cuf1*$^+$*/cuf1*$^+$, and *pat1-114/pat1-114 cuf1*Δ*/cuf1*Δ cells that were induced to undergo synchronous meiosis. Cells were either left untreated (−) or incubated in the presence of TTM (50 μM) or $CuSO_4$ (50 μM). At the indicated times after meiotic induction, *ctr4*$^+$, *ctr5*$^+$, and *act1*$^+$ (internal control) mRNA levels were analyzed in control strain (*cuf1*$^+$*/cuf1*$^+$) (*panels A* and *C*) and isogenic strain lacking the *cuf1*$^+$ alleles (*cuf1*Δ*/cuf1*Δ) (*panels B* and *D*).

using an anti-$His_5$ antibody due to the presence of an endogenous cluster that contains 5 His residues located within the N-terminal residues 10–14 of Cao1 (12). ChIP experiments were carried out as described previously (4).

## RESULTS

*ctr4*$^+$ *and ctr5*$^+$ *mRNA Levels Are Induced in Response to Low Levels of Copper in a Cuf1-dependent Manner in Early-phase Meiosis*—As previously observed (19) and as shown in Fig. 1, when a diploid parental strain *pat1-114/pat1-114* was synchronized through meiosis under copper-deficient conditions, *ctr4*$^+$ mRNA levels were induced ~16-fold compared with basal levels observed in untreated cells after 1 h of meiotic induction (Fig. 1). After 3 h of the meiotic program, *ctr4*$^+$ mRNA levels were reduced and subsequently repressed within ~5–7 h. RNA samples prepared from a *pat1-114/pat1-114 cuf1*Δ*/cuf1*Δ mutant strain showed loss of copper starvation-dependent induction of *ctr4*$^+$ gene expression (Fig. 1). A second member of the Ctr family, Ctr5, is known to assemble with Ctr4 to form the high affinity copper transport complex at the cell surface in fission yeast. Expression of the *ctr5*$^+$ gene was also analyzed as a function of time during meiosis (Fig. 1). Consistently, *ctr5*$^+$ mRNA levels were co-induced with the transcript levels of *ctr4*$^+$, except that they were lower than *ctr4*$^+$ levels. To further examine whether *ctr5*$^+$ transcription was controlled by Cuf1, a *pat1-114/pat1-114 cuf1*Δ*/cuf1*Δ deletion strain was incubated in the absence or presence of the copper chelator TTM (50 μM) or $CuSO_4$ (50 μM). As observed in the case of *ctr4*$^+$, deletion of *cuf1*$^+$ impaired the induction of *ctr5*$^+$ during meiosis (Fig. 1). We, therefore, concluded that *ctr4*$^+$ and *ctr5*$^+$ genes exhibit a similar meiotic temporal expression profile and that Cuf1 transcription factor is required for induction of both genes in response to copper starvation.

*The ctr6*$^+$ *Gene Is Transcriptionally Regulated by Cuf1 and Mei4 during Meiosis—ctr6*$^+$ encodes for a third member of the Ctr family in *S. pombe*. In cells proliferating in mitosis, its expression is induced under low levels of copper in a Cuf1-dependent manner (13). In contrast, *ctr6*$^+$ is negatively regulated when cells are exposed to exogenous copper. It is currently unknown whether *ctr6*$^+$ is expressed in meiotic cells. To investigate this question, *pat1-114/pat1-114* diploid cells were synchronously induced into meiosis and left untreated or were treated with either TTM (50 μM) or $CuSO_4$ (50 μM). Aliquots of cultures were taken after meiotic induction, and the steady-state levels of *ctr6*$^+$ mRNA were analyzed by RNase protection assays. Results showed that the steady-state levels of *ctr6*$^+$ mRNA under basal (untreated) and copper-starved (50 μM TTM) conditions were primarily increased between 3 and 9 h after meiotic induction (Fig. 2*A*). Surprisingly, in the presence of exogenous copper (50 μM), *ctr6*$^+$ transcript levels were detected after 5 h of meiotic induction but to a lesser extent in comparison with transcript levels observed in untreated cells (Fig. 2*A*). To assess whether Cuf1 was required for expression of *ctr6*$^+$ during meiosis, the *ctr6*$^+$ transcript was probed in a *pat1-114/pat1-114 cuf1*Δ*/cuf1*Δ mutant strain throughout meiosis. Under all conditions tested, disruption of *cuf1*$^+$ resulted in strongly reduced *ctr6*$^+$ mRNA levels (~4–12-fold) in comparison with those recorded in the case of wild-type cells grown under the same conditions (Fig. 2*B*). Weak *ctr6*$^+$ mRNA levels were primarily observed after 5 or 7 h of meiotic induction, which corresponds to the time of expression of several middle-phase genes. Because the meiotic transcription factor Mei4 is known to be required for the induction of several middle meiosis-specific genes (25), RNase protection assays were performed using a *pat1-114/pat1-114 mei4*Δ*/mei4*Δ mutant strain. Results were compared with those obtained with a *pat1-114/pat1-114* control strain. In the case of *mei4*Δ*/mei4*Δ cells, *ctr6*$^+$ transcript levels were only detected in response to copper starvation conditions and were absent under basal and copper-replete conditions (Fig. 2*C*). When a *cuf1*Δ*/cuf1*Δ *mei4*Δ*/mei4*Δ double mutant strain was examined, *ctr6*$^+$ transcript was not detected under all experimental conditions, including basal, copper-starved, and copper-replete conditions (Fig. 2*D*). Analysis of the *ctr6*$^+$ promoter revealed that it contains a putative consensus Mei4-binding FLEX sequence (40) and three Cuf1 binding CuSEs (Fig. 2*E*). To ascertain whether the FLEX element plays a role in *ctr6*$^+$ regulation during meiosis, we constructed a *ctr6*$^+$ promoter-*lacZ* fusion gene harboring a 620-bp fragment from the *ctr6*$^+$ promoter in which the three CuSEs elements have been mutagenized. Subsequently, we used this reporter construct that contained one FLEX element or the same promoter fragment in which the FLEX box has been

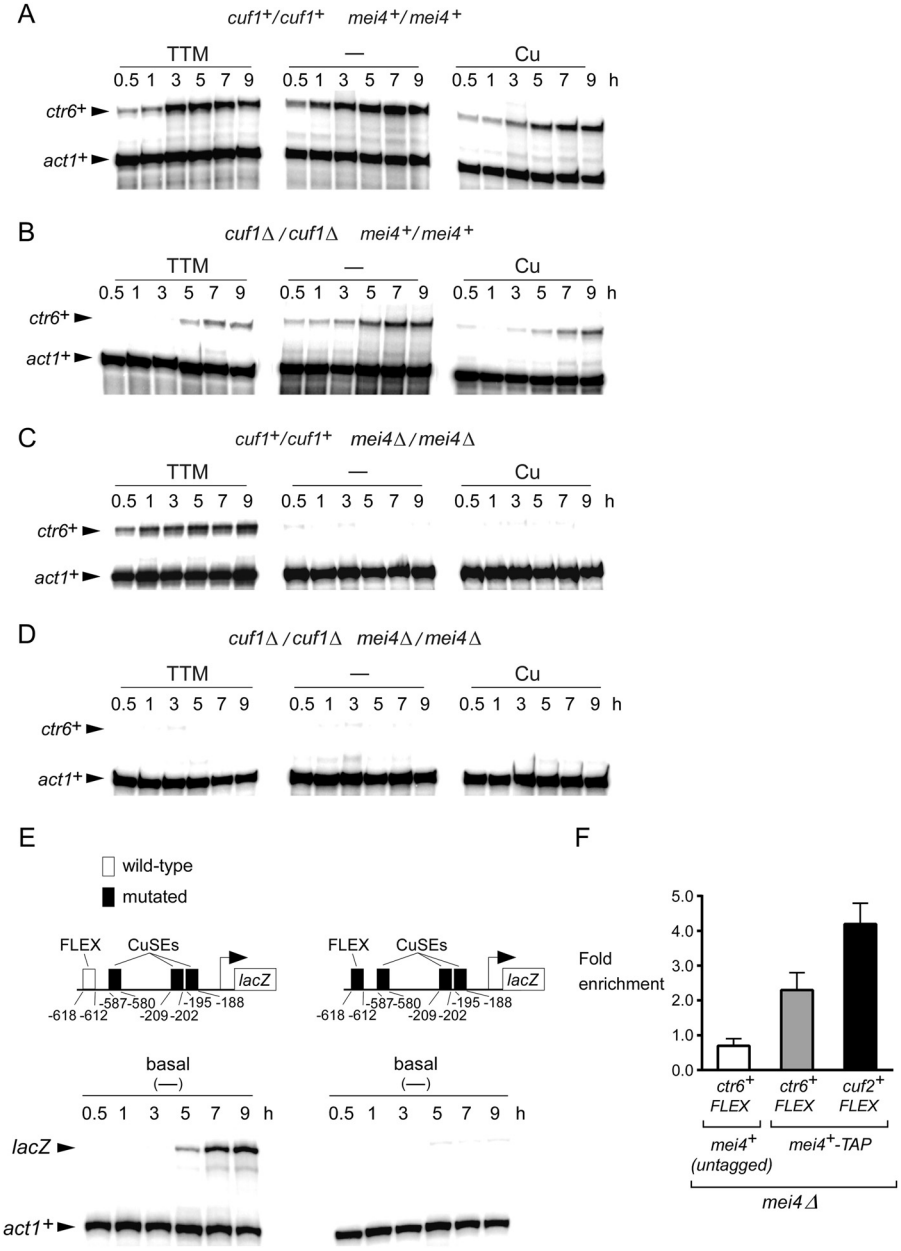


FIGURE 2. **Effect of cuf1Δ/cuf1Δ or mei4Δ/mei4Δ deletion on the expression of *ctr6*$^+$.** Cultures of *pat1-114/pat1-114 cuf1*$^+$*/cuf1*$^+$ *mei4*$^+$*/mei4*$^+$ (*panel A*), *pat1-114/pat1-114 cuf1Δ/cuf1Δ mei4*$^+$*/mei4*$^+$ (*panel B*), *pat1-114/pat1-114 cuf1*$^+$*/cuf1*$^+$ *mei4Δ/mei4Δ* (panel *C*), and *pat1-114/pat1-114 cuf1Δ/cuf1Δ mei4Δ/mei4Δ* (*panel D*) cells were induced to initiate and proceed through meiosis. Cells were left untreated (−) or incubated in the presence of TTM (50 $\mu$M) or $CuSO_4$ (50 $\mu$M). Total RNA was isolated from culture aliquots taken at the indicated time points. *ctr6*$^+$ and *act1*$^+$ steady-state mRNA levels were analyzed by RNase protection assays. *E*, diagram representation of a 620-bp *ctr6*$^+$ promoter DNA fragment and its mutant derivative that were fused upstream of the *lacZ* gene. The *white box* indicates the wild-type FLEX element, whereas the black ones represent mutant versions of FLEX and CuSEs elements. The nucleotide numbers refer to the positions of the *cis*-acting elements relative to that of the *ctr6*$^+$ initiator codon. Steady-state levels of *lacZ* and *act1*$^+$ mRNAs were analyzed at different time points after meiotic induction under basal conditions. *F*, ChIP assays were performed using untagged and TAP-tagged versions of Mei4. ChIP results are presented as the fold enrichment at the *ctr6*$^+$ or *cuf2*$^+$ promoter encompassing a FLEX element in comparison with a non-transcribed intergenic region. The data and *error bars* represent the average and S.D. from at least three biological replicates.

mutated. As shown in Fig. 2*E*, *ctr6*$^+$*-lacZ* expression from the reporter plasmid containing the FLEX box exhibited a meiotic gene time-dependent expression profile, peaking ~7–9 h after meiotic induction. In contrast, meiotic-dependent expression of *lacZ* mRNA was abrogated in the absence of the FLEX sequence. Furthermore, ChIP analysis showed that Mei4-TAP was enriched ~2.3-fold at the *ctr6*$^+$ promoter region encompassing the FLEX element in comparison with a non-transcribed intergenic region that served as a negative control (Fig. 2*F*). Untagged Mei4 immunoprecipitated only background levels of the *ctr6*$^+$ promoter region (~0.7-fold). Consistent with the fact that the Mei4 transcription factor is required for *cuf2*$^+$ gene expression during meiosis (26), Mei4-TAP occupied the *cuf2*$^+$ promoter with a ~4.2-fold enrichment (used as a positive control) (Fig. 2*F*). Taken together, these results indicate that the meiotic-dependent expression of *ctr6*$^+$ transcript requires both transcription factors, Cuf1 and Mei4, although Cuf1 has a greater contribution under copper-limiting conditions than Mei4.

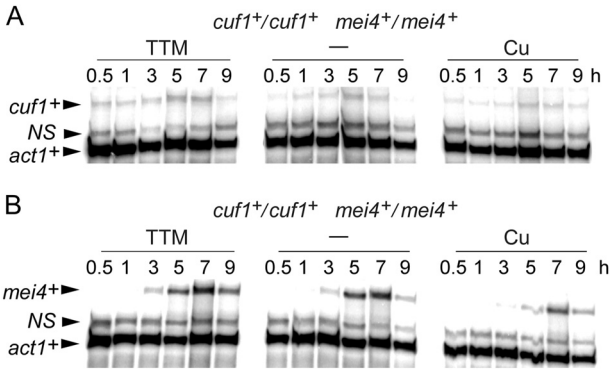


FIGURE 3. **Assessment of the mRNA steady-state levels of cuf1$^+$ and mei4$^+$ during meiosis.** *pat1-114/pat1-114 cuf1$^+$/cuf1$^+$ mei4$^+$/mei4$^+$* cells underwent synchronous meiosis under basal (-), copper-depleted, and copper-replete conditions. At the indicated time points, *cuf1$^+$*, *mei4$^+$*, and *act1$^+$* mRNA levels were analyzed by RNase protection assays. *NS,* non-specific signal.

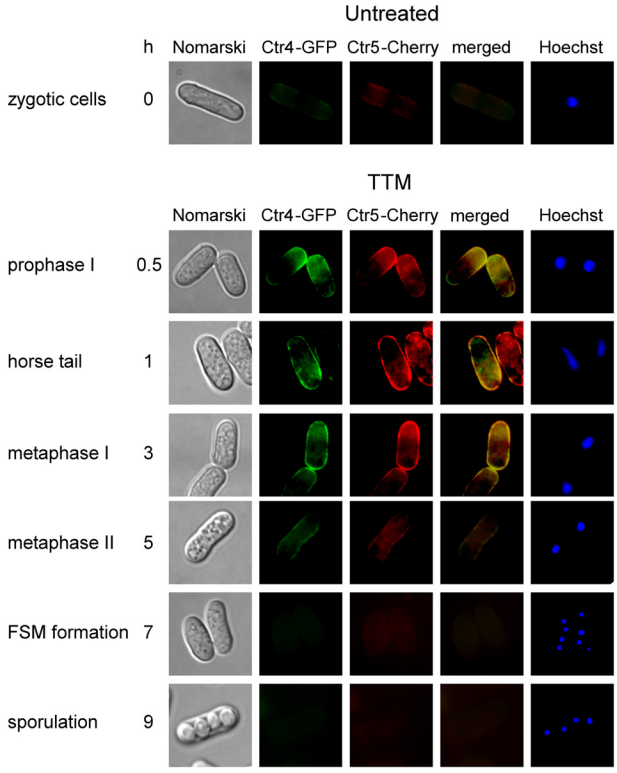


FIGURE 4. **Colocalization of Ctr4-GFP and Ctr5-Cherry during meiosis.** Diploid *h$^+$/h$^-$ ctr4Δ/ctr4Δ ctr5Δ/ctr5Δ* cells co-expressing functional *ctr4$^+$-GFP* and *ctr5$^+$-Cherry* alleles were induced to undergo azygotic meiosis. Once induced, cells were differentiated in the presence of 50 $\mu$M TTM. Fluorescence signals of Ctr4-GFP and Ctr5-Cherry were observed at different stages of meiosis (*center left*). The merged images are shown in the *center right panels*. Nomarski optics (*far left*) were used to ascertain cell morphology and Hoechst 33342 staining to visualize DNA (*far right*). *FSM*, forespore membrane.

*cuf1$^+$ and mei4$^+$ Gene Expression Profiles as a Function of Changes in Copper Levels during Meiosis*—We next analyzed steady-state mRNA levels of *cuf1$^+$* and *mei4$^+$* as a function of copper availability during meiosis. A *pat1-114/pat1-114* diploid strain was synchronized to initiate and proceed through the meiotic program. Before their entry into meiosis, cells were left untreated or exposed to TTM (50 $\mu$M) or $CuSO_4$ (50 $\mu$M). Aliquots of cultures were picked up at distinct time points after meiotic induction, and steady-state levels of *cuf1$^+$* and *mei4$^+$* mRNAs were analyzed by RNase protection assays. Results showed that *cuf1$^+$* and *mei4$^+$* transcripts were detected under basal, copper-starved, or copper-replete conditions (Fig. 3). *cuf1$^+$* mRNAs were seen at each time point and were slightly increased after 5 and 7 h of meiotic induction (~2–3-fold compared with levels observed after 1 h of meiotic induction). In the case of *mei4$^+$* mRNAs, their steady-state levels were absent after 1 h of meiotic induction. Subsequently, a slight increase of *mei4$^+$* expression was observed after 3 h, and it became more pronounced 5 and 7 h after meiotic induction (Fig. 3). After cell entrance into meiosis, the expression profile of *mei4$^+$* revealed that it reached a maximum 5–7 h after meiotic induction, indicating that its presence was primarily required during the middle meiotic phase. In the case of *cuf1$^+$*, its expression profile as a function of time suggested a broader role during the differentiation process. In response to copper (50 $\mu$M), *cuf1$^+$* and *mei4$^+$* were expressed to a slightly lesser degree overtime. However, their overall expression profiles were unchanged as compared with those observed under basal and copper-depleted conditions (Fig. 3). This observation was likely related to a general effect of copper on meiosis instead of a specific effect of copper on *cuf1$^+$* and *mei4$^+$* transcripts.

*Ctr4-GFP and Ctr5-Cherry Colocalize at the Cell Surface during the First Stages of Meiosis*—When cells grow mitotically under low levels of copper, Ctr4 and Ctr5 colocalize at the plasma membrane where they form a heteroprotein complex, which mediates high affinity copper transport (5, 6). Our previous studies reported location of Ctr4 at the plasma membrane shortly after induction of meiosis (19). After 3 h of meiotic induction, Ctr4-GFP-associated fluorescence progressively disappeared, a result that was consistent with decreased *ctr4$^+$* mRNA levels at the same stage of the meiotic program. To further characterize the location of Ctr4 and Ctr5 during meiosis, functional *ctr4$^+$-GFP* and *ctr5$^+$-Cherry* alleles were integrated into *h$^-$ ctr4Δ ctr5Δ* and *h$^+$ ctr4Δ ctr5Δ* cells. After mating, *h$^-$/h$^+$ ctr4Δ/ctr4Δ ctr5Δ/ctr5Δ ctr4$^+$-GFP/ctr4$^+$-GFP ctr5$^+$-Cherry/ctr5$^+$-Cherry* diploid cells were cultured to undergo azygotic synchronous meiosis. Under copper-limiting conditions (50 $\mu$M TTM), Ctr4-GFP and Ctr5-Cherry fluorescent proteins were rapidly co-detected, exhibiting fluorescence in prophase I, horse tail, and metaphase I (Fig. 4). At metaphase II, the Ctr4-GFP and Ctr5-Cherry fluorescent signals progressively decreased and then virtually disappeared during forespore membrane formation and sporulation (Fig. 4). Consistent with the existence of a clear interdependence between Ctr4 and Ctr5, the Ctr4-GFP- and Ctr5-Cherry-associated fluorescent signals were consistently co-localized (Fig. 4). Because transcription of the *ctr4$^+$-GFP* and *ctr5$^+$-Cherry* genes were repressed under high copper conditions (50 $\mu$M $CuSO_4$), there was an absence of fluorescent signals in copper-treated zygotic cells (data not shown). Collectively, microscopic analyses of meiotic cells revealed that Ctr4-GFP and Ctr5-Cherry fusion proteins co-localize with each other. Furthermore, these two proteins were observed at the cell surface within 30 min after meiotic induction and remained at the cell periphery until the first meiotic division occurs.

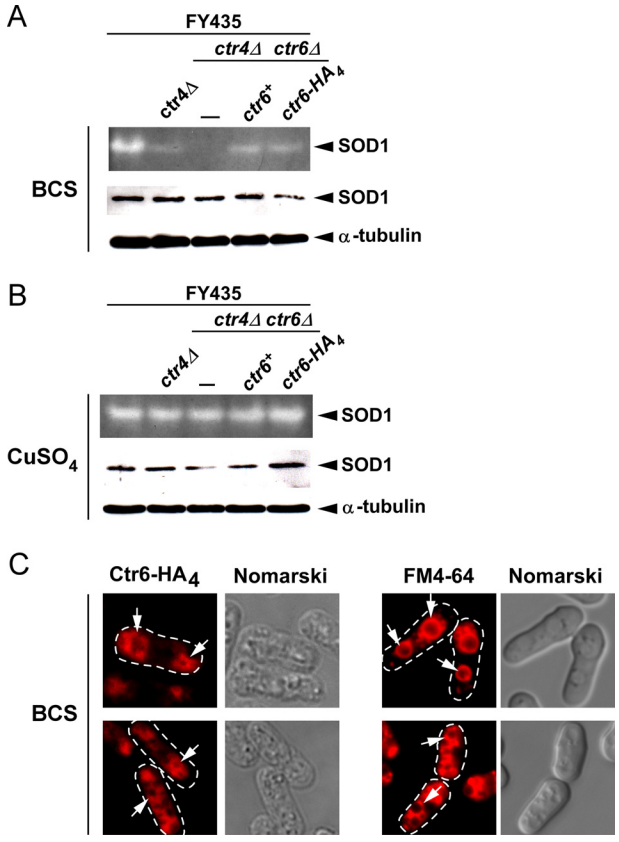


FIGURE 5. **The vacuolar copper transporter Ctr6 contributes to production of active SOD1 during mitosis.** *A,* representative in-gel activity assay of *S. pombe* strain (FY435) harboring a disrupted *ctr4*Δ allele exhibiting strong reduction of SOD1 activity under low copper conditions (100 $\mu$M BCS). Under the same conditions, a *ctr4*Δ *ctr6*Δ double mutant strain was devoid of measurable SOD1 activity unless the $ctr6^+$ or $ctr6^+$-$HA_4$ allele was returned by integration. Protein extracts prepared from these strains were analyzed for steady-state levels of SOD1 by immunoblotting using anti-SOD1 and anti-α-tubulin antibodies. *B,* SOD1 activity and steady-state protein levels were determined in the same strains of *panel A* in the presence of excess $CuSO_4$ (50 $\mu$M). *C,* cells were analyzed by indirect immunofluorescence microscopy for vacuolar localization of a functional Ctr6-$HA_4$ fusion protein that was expressed in *ctr4*Δ *ctr6*Δ cells grown under copper-limiting conditions (100 $\mu$M BCS) (*left*). FM4–64 staining (*right*) was visualized by fluorescence microscopy as a marker of vacuolar membranes. Nomarski optics were used to examine cells under fixed (*left*) and non-fixed (*right*) conditions. *White arrows* indicate examples of vacuolar membranes.

*A Functional Vacuolar Ctr6 Transporter Is Required for the Production of a Fully Active SOD1*—As previously observed (13) and as shown in Fig. 5*A*, cells harboring a double deletion of $ctr4^+$ and $ctr6^+$ (*ctr4*Δ *ctr6*Δ) are defective in SOD1 activity under copper starvation conditions. Loss of endogenous SOD1 activity was restored to ~40% that of wild-type parental strain (FY435) by the addition of exogenous copper (50 $\mu$M $CuSO_4$) (Fig. 5*B*). Under low copper conditions, disruption of the $ctr4^+$ gene (*ctr4*Δ) dramatically reduced SOD1 activity, resulting in a weak, but significant proportion of SOD1 activity that reflected the contribution of Ctr6 in activating SOD1 (Fig. 5*A*). This result was used as a positive control to test whether *ctr4*Δ *ctr6*Δ cells expressing an untagged or $HA_4$-tagged $ctr6^+$ allele could acquire levels of SOD1 that were comparable with those found in the *ctr4*Δ strain. Results showed that Ctr6-$HA_4$ functionally complemented SOD1 deficiency of the double *ctr4*Δ *ctr6*Δ mutant strain at the same level as did untagged Ctr6 (Fig. 5*A*). We then used *ctr4*Δ *ctr6*Δ cells expressing the Ctr6-$HA_4$ fusion protein under low copper conditions and performed indirect immunofluorescence microscopy using anti-HA antibody. Results showed that Ctr6-$HA_4$ localized to the membrane of vacuoles in cells proliferating in mitosis under copper-limiting conditions (Fig. 5*C*). Conveniently, when $ctr6^+$-$HA_4$ was induced by copper starvation, the number and size of the vacuoles decreased and became bigger in size, respectively, as a consequence of nutrient limitation (data not shown) (13), facilitating Ctr6-$HA_4$ localization. To further confirm that Ctr6-$HA_4$-associated fluorescence was detected in the vacuole membranes of cells, the vacuole-staining dye FM4–64 was used as a marker. Ctr6-$HA_4$ and FM4–64 exhibited similar subcellular localization patterns within the cells (Fig. 5*C*). Because the vacuole has been shown to play an important role for metal ion storage (14, 37–39), one model has proposed that Ctr6 mobilizes stores of copper from the organelle to provide it to SOD1, thereby contributing to its activation (13).

*Analysis of Ctr6 Localization during Meiotic Program*—To further investigate the role of Ctr6 during meiosis, a functional $ctr6^+$-$HA_4$ allele was integrated into $h^-$ *ctr6*Δ and $h^+$ *ctr6*Δ cells. After mating, $h^-/h^+$ *ctr6*Δ/*ctr6*Δ $ctr6^+$-$HA_4$/$ctr6^+$-$HA_4$ diploid cells were cultured under conditions to induce azygotic synchronous meiosis. Under basal or low copper conditions, Ctr6-$HA_4$ was detected in the vacuole membranes of cells at prophase I (data not shown) and metaphase I (3-h time point) (Fig. 6). At the 3-h time point, Ctr6-$HA_4$-associated fluorescence was more prominent in cells starved for copper compared with cells incubated under basal conditions. When azygotic meiosis was synchronously induced in the presence of copper, Ctr6-$HA_4$ fluorescent signal was barely detected during the first 3 h of meiosis (Fig. 6). During meiotic metaphase II (5-h time point) and forespore membrane formation (7-h time point), zygotic cells displayed Ctr6-$HA_4$ fluorescence in smaller vacuole or vesicle membranes. At these stages the strength of the fluorescent signals was strong regardless of copper conditions. After 9 h of meiotic induction (sporulation), Ctr6-$HA_4$ generated a fluorescent signal at the spore membrane, suggesting a novel role for the Ctr6 transporter at the spore surface. To validate that Ctr6-$HA_4$ located at the forespore membrane during late meiosis, we analyzed (under the same conditions) cells expressing a GFP-Psy1 protein, an intrinsic component of forespore membrane. Both proteins exhibited similar fluorescent patterns (Fig. 6). Additional evidence supporting the presence of Ctr6 at the membrane of spores was obtained by findings that Ctr6-$HA_4$-associated fluorescence was detected at the surface of spores that had been newly released from asci after 12 h of meiotic induction (Fig. 6). Taken together, data from microscopic analysis of meiotic cells revealed that a functional Ctr6-$HA_4$ protein localizes in the vacuole membranes of cells that had undergone meiotic divisions and that it becomes resident of the spore membrane during the forespore membrane formation.

*Ctr4 and Ctr6 Are Required for the Synthesis of Fully Active SOD1, whereas an Additional Contribution by Mfc1 Is Necessary for Full Activation of CAO in Late-phase Meiosis*—To determine whether Ctr4 or Ctr6 were required for providing copper to SOD1 during meiosis, we used isogenic diploid

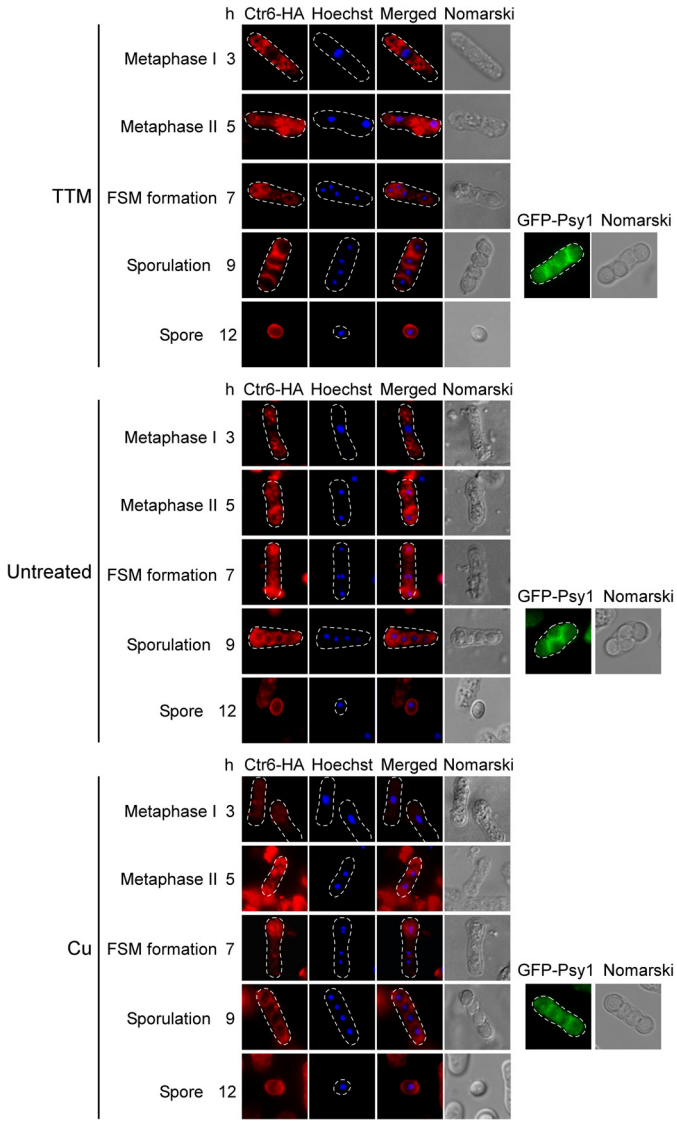


FIGURE 6. **Subcellular localization of Ctr6-*HA*$_4$ during meiosis and sporulation.** *h*$^-$/*h*$^+$ *ctr6Δ/ctr6Δ* mutant cells expressing Ctr6-*HA*$_4$ were synchronously induced to undergo azygotic meiosis and then were left untreated or were treated with TTM (50 $\mu$M) or $CuSO_4$ (Cu) (50 $\mu$M) for the indicated time points. Hoechst 33342 staining was used to visualize DNA (*center left*). The merged images of the Ctr6-*HA*$_4$ and the Hoechst dye are shown (*center right*). Fixed cells observed by indirect immunofluorescence (Ctr6-*HA*$_4$; *far left*) were also examined by Nomarski optics (*far right*). After 9 h of meiotic induction, the GFP-Psy1 fluorescent protein was examined and used as a forespore membrane resident marker. At the 12-h time point, the Ctr6-*HA*$_4$ fluorescent signal was observed on the membrane of spores that were newly released from asci. *FSM*, forespore membrane.

strains harboring wild-type genes or insertionally inactivated *ctr4Δ*/*ctr4Δ*, *ctr6Δ*/*ctr6Δ* (Fig. 7) or *ctr4Δ ctr6Δ*/*ctr4Δ ctr6Δ* alleles (Fig. 8). In the presence of TTM (25 $\mu$M), *ctr4Δ*/*ctr4Δ* cells exhibited SOD1 activity that was significantly lower (~5.3-fold) than that of wild-type cells (Fig. 7). In the case of *ctr6Δ*/*ctr6Δ* cells, SOD1 activity was less (~2.2-fold) than that of the wild-type cells but higher (~2.4-fold) than that of *ctr4Δ*/*ctr4Δ* cells (Fig. 7). Under copper starvation conditions (25 $\mu$M TTM), no measurable SOD1 activity was observed in the case of *ctr4Δ ctr6Δ*/*ctr4Δ ctr6Δ* double mutant strain (Fig. 8), revealing a critical role for both Ctr4 and Ctr6 in conferring SOD1 activity during meiosis. To verify that the SOD1 protein was present in wild-type and mutant strains, total protein extracts were analyzed by immunoblotting at the indicated meiotic time points (Figs. 7 and 8). Results showed that detectable levels of SOD1 protein were present in all strains, indicating that the decrease or lack of activity was not due to the absence of SOD1 expression. As expected, SOD1 activity could be restored by the addition of high exogenous copper concentrations (25 $\mu$M) to the cell cultures (Figs. 7 and 8). This effect was likely due to the fact that copper ions were taken up by way of a low-affinity copper transport system, thereby bypassing requirements for high-affinity copper transporters.

The above-mentioned strains were also used to monitor CAO activity during meiosis. Two genes encode members of the CAO family in *S. pombe*. However, only one gene (*cao1*$^+$) encodes an active enzyme (12). Diploid wild-type cells were synchronized through meiosis in the presence of either TTM (25 $\mu$M) or $CuSO_4$ (25 $\mu$M). Under copper-limiting conditions, results showed that levels of CAO activity increased as a function of time to reach maximal activity within 6 h, at which point CAO activity levels remained high until the end of the meiotic program (Figs. 7 and 8). In the case of *ctr4Δ/ctr4Δ* mutant cells they exhibited an activity ~3–3.7-fold weaker than wild-type cells after 1 h of meiotic induction under low copper conditions (Fig. 7). Although CAO activity slightly increased after 3 and 6 h of meiotic induction, *ctr4Δ/ctr4Δ* null cells displayed an activity that was ~3.1–3.6-fold weaker than that of wild-type cells. After the 6-h time point, we observed that CAO activity levels were significantly up-regulated (~27%), although this increase was insufficient to reach levels observed in the case of wild-type cells (Fig. 7). After 1 h of meiotic induction, copper-starved *ctr6Δ/ctr6Δ* mutant cells exhibited CAO activity comparable with that of the wild-type strain (Fig. 7). However, levels of CAO activity were quickly reduced ~4.9-fold within the next 3 h (Fig. 7). Results showed that CAO activity increased after 6 h of meiotic induction (~3-fold compared with levels observed after 3 h of meiotic induction). This increased activity was followed by a second increase (~2.4-fold compared with levels after 6 h of meiotic induction) within 9 h of TTM treatment (Fig. 7). CAO activity of *ctr4Δ/ctr4Δ* and *ctr6Δ/ctr6Δ* cells was restored by supplementing the medium with 25 $\mu$M exogenous copper (Fig. 7). This effect was likely due to mobilization of copper via a low-affinity copper uptake system, which bypasses the requirement for Ctr4 and Ctr6 transport systems. To ensure that the decrease of CAO activity in the *ctr4Δ/ctr4Δ* and *ctr6Δ/ctr6Δ* mutant strains grown under low copper conditions was not due to a defect in Cao1 expression, we analyzed the steady-state protein levels of Cao1 by immunoblotting. We found that Cao1 was produced at similar steady-state levels in wild-type and mutant strains (data not shown).

Once early-phase meiosis has been initiated under conditions of copper starvation (25 $\mu$M TTM), *ctr4Δ ctr6Δ*/*ctr4Δ ctr6Δ* double mutant cells exhibited a decrease in CAO activity that was reminiscent of cells bearing a single *ctr4Δ* deletion (~4.2-fold weaker activity compared with wild-type strain) (Fig. 8). This was followed by a modest increase of CAO activity after 3 h (~2.1-fold) and 6 h (~1.2-fold) of meiotic induction in comparison with double mutant cells at the 1- and 3-h time points, respectively. As observed in the case of *ctr4Δ/ctr4Δ*

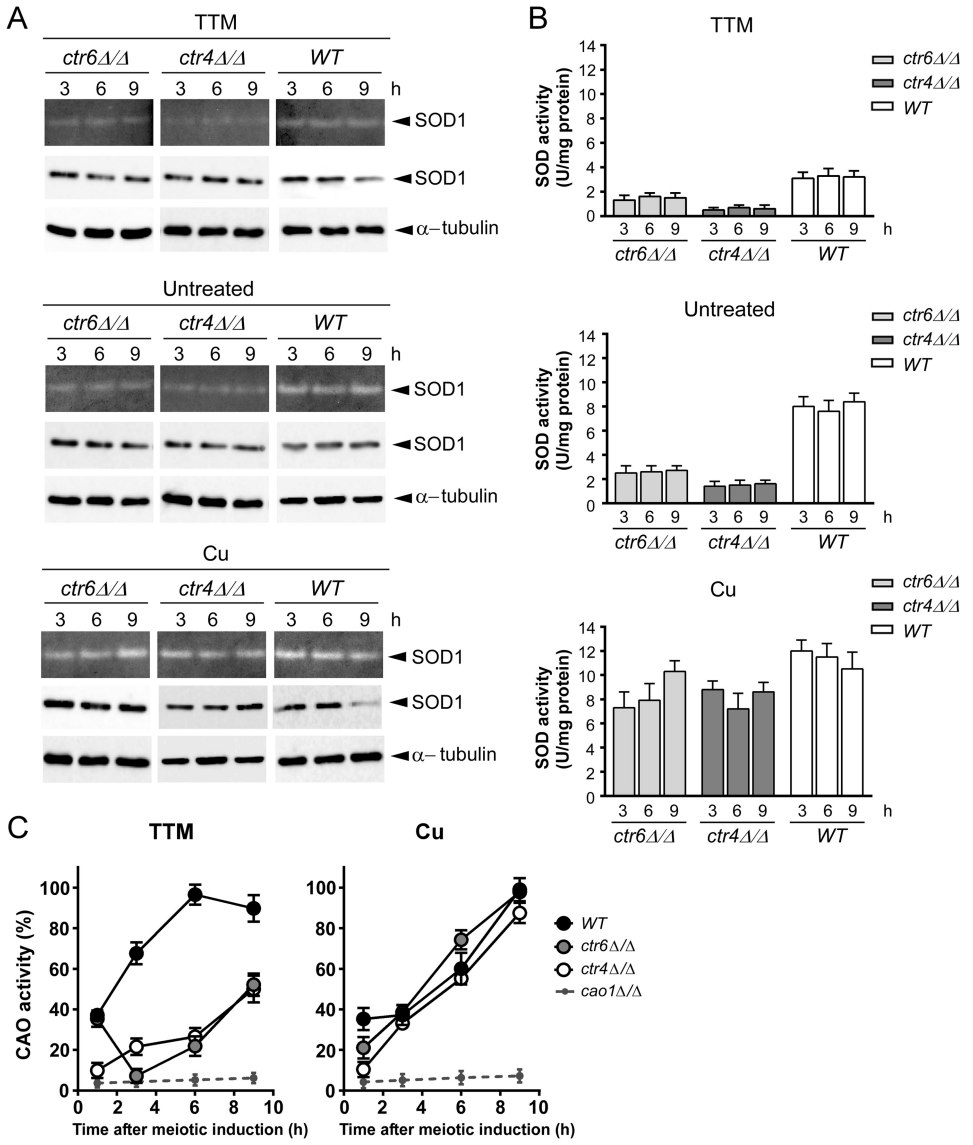


FIGURE 7. **Effect of ctr4Δ/ctr4Δ and ctr6Δ/ctr6Δ disruptions on SOD1 and CAO activities during meiosis.** *A*, wild-type diploid ($h^-/h^+$ *ctr4*$^+$/*ctr4*$^+$ *ctr6*$^+$/*ctr6*$^+$), $h^-/h^+$ *ctr6*Δ/*ctr6*Δ, and $h^-/h^+$ *ctr4*Δ/*ctr4*Δ mutant strains were synchronously induced to undergo meiosis under basal (untreated), copper-depleted (25 μM TTM), and copper-replete (25 μM $CuSO_4$) conditions. At the indicated time points total extracts from aliquots of cultures were analyzed for SOD1 activity using an in-gel activity assay. Protein extracts were analyzed for steady-state protein levels of SOD1 and α-tubulin by immunoblotting using anti-SOD1 and anti-α-tubulin antibodies, respectively. *B*, spectrophotometric determination of SOD activity was also performed from these strains using a cytochrome *c*/xanthine oxidase method. Data are the averages of triplicate determinations ± S.D. *C*, the above-mentioned strains plus a $h^-/h^+$ *cao1*Δ/*cao1*Δ mutant were analyzed for CAO activity by spectrophotometric assays using 4-aminoantipyrine and vanillic acid. *Error bars* indicate S.D. of activities from samples analyzed in triplicate.

mutant strain, CAO activity levels of *ctr4*Δ *ctr6*Δ/*ctr4*Δ *ctr6*Δ mutant cells were markedly up-regulated (~39%) between 6 and 9 h, suggesting that another protein participated in delivering copper to Cao1. Because previous results had shown that Mfc1 was required for production of fully active CAO during meiosis (19), a *ctr4*Δ *ctr6*Δ *mfc1*Δ/*ctr4*Δ *ctr6*Δ *mfc1*Δ triple mutant was generated and induced to undergo synchronous meiosis. After 9 h of meiotic induction, results showed that inactivation of *mfc1*$^+$ (*mfc1*Δ) in the context of *ctr4*Δ *ctr6*Δ resulted in ~43 and ~79% less CAO activity as compared with *ctr4*Δ *ctr6*Δ/*ctr4*Δ *ctr6*Δ double mutant and wild-type cells, respectively. Consistent with the restoration of CAO activity after the addition of exogenous copper (25 μM), double and triple mutant strains displayed an increase in CAO activity up to ~93 and ~82% of the levels observed in the case of wild-type strain, respectively (Fig. 8). To ensure that the decrease of CAO activity in mutant strains grown under copper-limiting conditions was not due to a defect in CAO expression, steady-state levels of Cao1 were analyzed and found to remain present at similar levels throughout the entire period of meiosis in all strains (data not shown). Taken together, the results revealed a distinct requirement of copper transporters for activation of SOD1 and CAO enzymes under conditions of copper starvation during meiosis. Whereas Ctr4 and Ctr6 transporters are required to produce a fully active SOD1 enzyme, the presence of the additional transporter Mfc1 is needed to ensure maximal CAO activity throughout the entire meiotic program.

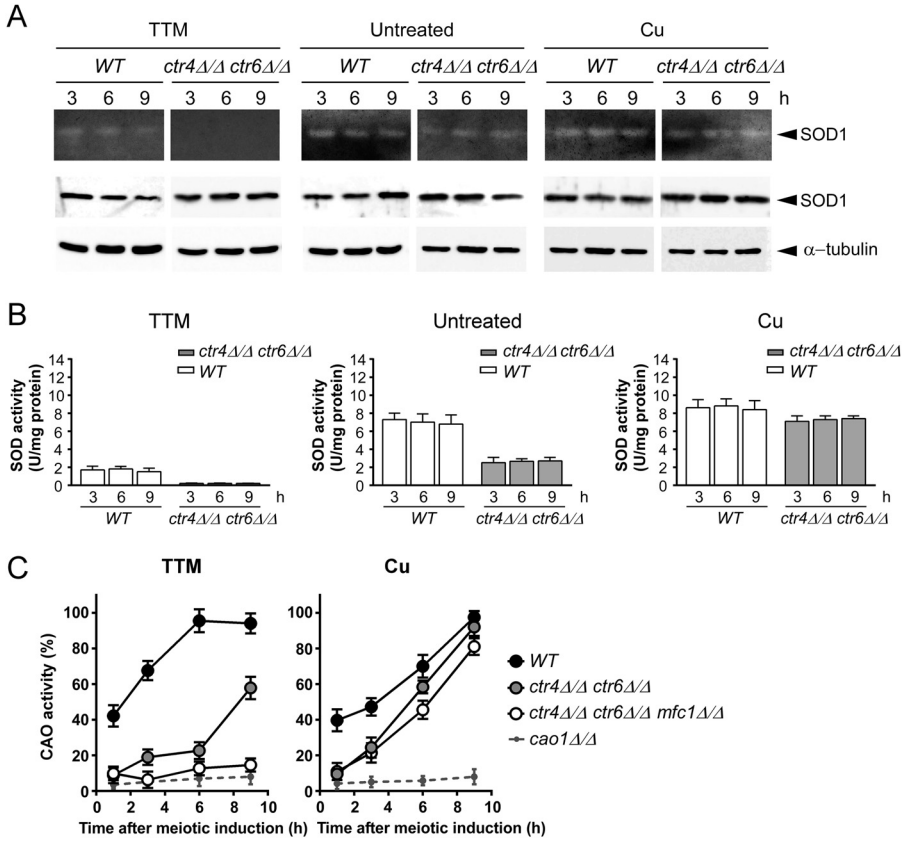


FIGURE 8. **SOD1 and Cao1 enzymes require different combinations of copper transporters for their activation during meiosis.** Cultures of $h^-/h^+$ *ctr4*$^+$/*ctr4*$^+$ *ctr6*$^+$/*ctr6*$^+$ (*WT*) and $h^-/h^+$ *ctr4*Δ/*ctr4*Δ *ctr6*Δ/*ctr6*Δ diploid cells were synchronously induced into meiosis under basal (untreated), copper-starved (25 $\mu$M TTM), or copper-replete (25 $\mu$M $CuSO_4$) conditions. Total extracts were prepared from culture aliquots taken at the indicated time points. SOD1 activity was determined using an in-gel assay. Aliquots of total-extract preparations were also examined by immunoblotting using either anti-SOD1 or anti-α-tubulin antibody. *B*, cell extracts were prepared from strains used in *A*, and analyzed by a cytochrome *c*/xanthine oxidase method. Results are the averages of triplicate determinations ± S.D. *C*, FY435/FY436 ($h^+/h^-$) (*WT*), $h^+/h^-$ *ctr4*Δ/*ctr4*Δ *ctr6*Δ/*ctr6*Δ, $h^+/h^-$ *ctr4*Δ/*ctr4*Δ *ctr6*Δ/*ctr6*Δ *mfc1*Δ/*mfc1*Δ, and $h^+/h^-$ *cao1*Δ/*cao1*Δ strains were synchronously induced into azygotic meiosis under copper-starved or copper-replete conditions. CAO activity was quantitated in cell lysates at the indicated time after meiotic induction. Data are the averages of triplicate determinations ± S.D.

## DISCUSSION

The biosynthesis of copper transporters Ctr4 and Ctr5 is dependent on the presence of the copper-sensing transcription factor Cuf1, which itself is activated under low-copper conditions during the mitotic cell cycle (5, 11, 33). Under these conditions, Ctr4 and Ctr5 are co-expressed and are assembled as a heteromeric complex at the cell surface where it mediates high affinity copper transport. When cells switch from mitosis to meiosis, expression profiles of *ctr4*$^+$ and *ctr5*$^+$ revealed that the two genes are still co-expressed and co-localized at the cell surface but only during the early steps of the meiotic program. Once pre-meiotic DNA replication and recombination are completed, both transcript and protein levels of Ctr4 and Ctr5 decrease progressively, suggesting that high affinity copper transport mediated by the Ctr4-Ctr5 complex is primarily needed in early meiosis. Possible explanations may be that one or more copper-dependent enzyme(s) is required for early steps of meiosis or copper ions need to be transported with very high efficacy from the environment during early meiosis, thereby allowing storage for subsequent usage during middle and late meiosis. As observed in the case of mitotic cells, expression of *ctr4*$^+$ and *ctr5*$^+$ in meiotic cells was copper starvation- and Cuf1-dependent. During meiosis, *ccc2*$^+$ that encodes a putative copper-transporting P-type ATPase exhibited a constitutive transcription as a function of time or copper needs during meiosis (data not shown), eliminating any correlation between changes in expression profiles of *ctr4*$^+$/*ctr5*$^+$ genes and transcriptional levels of *ccc2*$^+$.

In the case of *cuf1*$^+$, its meiotic expression profile differed from that of *ctr4*$^+$ and *ctr5*$^+$. Although *cuf1*$^+$ mRNA levels were detected in early meiosis, its transcript levels remained expressed throughout the meiotic division and spore maturation processes. They were slightly increased 5 and 7 h after meiotic induction, which corresponds to the end of the second meiotic division and the biogenesis of forespore membrane. The fact that the expression of *cuf1*$^+$ was sustained throughout the meiotic program suggested the existence of additional Cuf1-dependent target genes along with *ctr4*$^+$ and *ctr5*$^+$. One candidate gene was *ctr6*$^+$, as its mitotic copper-dependent expression is regulated by Cuf1 (13). Furthermore, as opposed to the expression profiles of *ctr4*$^+$ and *ctr5*$^+$, *ctr6*$^+$ transcripts were detected during early, middle, and late phases of meiosis. The nature of the mechanism by which Cuf1 stops to activate *ctr4*$^+$ and *ctr5*$^+$ after early meiosis but still activates *ctr6*$^+$ during middle and late phases is unknown. Nonetheless, deletion of *cuf1*$^+$ (*cuf1*Δ/*cuf1*Δ) led to a substantial decrease of *ctr6*$^+$

mRNA levels. Surprisingly, its expression was not completely abolished and remained detectable during and after meiotic divisions. On the basis of this observation, *ctr6*$^+$ expression was analyzed in a *mei4*Δ*/mei4*Δ mutant strain, which lacks the transcription regulator Mei4 that is required for the induction of several middle meiosis-specific genes (25). The results showed that *ctr6*$^+$ transcription relies on Mei4 during the meiotic divisions and the process of spore formation, especially under basal and copper-replete conditions. These observations led to the conclusion that meiotic differentiation requires a dual regulation of *ctr6*$^+$ by two distinct transcription factors and that ensures the continuous presence of Ctr6 during the developmental program.

In cells undergoing vegetative growth (mitosis), Ctr6 localizes to the vacuolar membrane under conditions of low copper availability. After cell entry into meiosis, microscopic analyses revealed that Ctr6 localized to the vacuolar membrane before completion of the first meiotic division. After completion of meiosis I, Ctr6 intracellular distribution had the appearance of cytoplasmic vesicular staining within the zygote. After the second meiotic division, zygotic cells exhibited Ctr6 fluorescence as large vesicular structures that appeared to progressively surround the chromosomal material. After forespore membrane closure, Ctr6 resided at the prespore membrane in which the chromosomal DNA is packed. On the basis of these observations, we propose that Ctr6 moves from the vacuolar membrane to the forespore membrane over the course of the meiotic program. Another *S. pombe* protein, Psy1, has been reported to be differentially located in cells proliferating in mitosis as opposed to meiosis (41). In the case of Psy1, it localizes to the plasma membrane in mitotic cells but to the forespore membrane of developing asci (42). Previous experiments using the fluorescent copper binding tracker Coppersensor-1 (43, 44) have shown that forespores accumulate labile cellular copper in sporulating cells (19). This observation was consistent with a need for translocation of Ctr6 from the vacuolar membrane to the forespore membrane. Ctr6 may transport stored copper from the prespore to the cytosol where meiotic copper-dependent enzymes can be found such as the SOD1 (data not shown). It is known that the forespore membrane expands by membrane vesicle fusion. Studies have reported that these vesicles are derived from the endoplasmic reticulum via the Golgi network (41, 46–48). However, recent studies have shown that vacuolar proteins participate in forespore membrane assembly and may involve vacuolar membranous structures for forespore membrane formation (49, 50). This mechanism may contribute to relocation of Ctr6 to the nascent forespore membrane where it would serve to mobilize intracellular pools of labile copper. The localization of Ctr6 on the spore membrane at the end of sporulation may also suggest a role for Ctr6 in spore germination. In agreement with this possibility, we have observed that isolated spores from *ctr6*Δ*/ctr6*Δ asci exhibited a decrease in viability as compared those of *ctr6*$^+$*/ctr6*$^+$ when returned for germination under low-copper conditions (data not shown).

To characterize the functional importance of the presence of Ctr4 and Ctr6 during meiosis, copper-dependent SOD1 and CAO activities were monitored during spore formation. Results showed that under conditions of copper starvation, cells lacking Ctr4 (*ctr4*Δ) exhibited a dramatic decrease in SOD1 activity compared with that of wild-type cells. Under the same conditions, a *ctr6*Δ single mutant displayed less SOD1 activity, but the decrease was less pronounced compared with a *ctr4*Δ single mutant. In copper-starved *ctr4*Δ *ctr6*Δ double mutant cells, SOD1 activity was undetectable, suggesting that both Ctr4 and Ctr6 represent two key players for delivering copper to SOD1 during meiosis. The fact that Ctr4 and Ctr6 exhibited a distinct meiotic temporal expression profile may help to ensure a constant source of copper for SOD1. In *S. cerevisiae* it has been reported that sporulation in homozygous *sod1*Δ*/sod1*Δ diploids is decreased ~100-fold in comparison with homozygous wild-type (*SOD1/SOD1*) diploids (45), suggesting an important role of SOD1 in meiosis. In addition to scavenging reactive superoxide anions that are produced during meiosis, SOD1 may participate in other functions that are required during meiotic differentiation. On the basis of the results, we conclude that SOD1 must already be active or rapidly activated after induction of meiosis and that Ctr4 and Ctr6 play an important role in delivering copper to SOD1 for its activation.

To further analyze the relative contribution of Ctr4 and Ctr6 during meiosis, CAO activity was analyzed in wild-type and *ctr4*Δ*/ctr4*Δ, *ctr6*Δ*/ctr6*Δ and *ctr4*Δ *ctr6*Δ*/ctr4*Δ *ctr6*Δ mutant cells. After induction of meiosis under low-copper conditions, we observed that the presence of Ctr4 was required for providing copper to Cao1 (the sole active CAO in *S. pombe*) at the initial stage of meiosis. Although the presence of Ctr6 was also important, its contribution was not detected at the same time in comparison with that of Ctr4, and was mainly seen after 3 h of meiotic induction. Intriguingly, but consistently with its meiotic temporal expression profile (19), the meiosis-specific copper transporter Mfc1 participated in the production of active CAO but only after 6 h of meiotic induction. Taken together, our results argue in favor of a model in which the three copper transporters Ctr4, Ctr6, and Mfc1 participate in the delivery of copper to CAO in a time-dependent manner, thereby ensuring that an active CAO is present throughout the entire meiotic program. One can envision that Ctr4, which is a major component of the heteromeric Ctr4-Ctr5 complex at the cell surface during the early stages of meiosis, plays a critical role for the acquisition of the primary pool of copper from the environment. When the Ctr4-Ctr5 heterocomplex is no longer present at the cell surface, Ctr6 serves to mobilize intravacuolar stores of copper, participating in the delivery of copper to cytosolic copper-dependent enzymes. After forespore membrane closure, Mfc1 would mediate copper accumulation into prespores, participating in the activation of Cao1 that localizes to the spore at this meiotic stage. During the sporulation process, a proportion of Ctr6 migrates from the vacuole to the forespore membrane where its presence may be required to counterbalance the action of Mfc1, therefore, ensuring that a fraction of copper could be delivered in the cytoplasmic region of the ascus. Although future studies will be required to demonstrate this model, results presented here are consistent with the existence of a dynamic interplay between the copper transport systems during meiosis of *S. pombe*.

*Acknowledgments—We are grateful to Dr. Gilles Dupuis for critically reading the manuscript and for valuable comments. We thank Raymund Wellinger for the use of the micromanipulator in the tetrad dissections.*

## REFERENCES


1. Nevitt, T., Ohrvik, H., and Thiele, D. J. (2012) Charting the travels of copper in eukaryotes from yeast to mammals. *Biochim. Biophys. Acta* **1823,** 1580–1593
2. Beaudoin, J., Ekici, S., Daldal, F., Ait-Mohand, S., Guérin, B., and Labbé, S. (2013) Copper transport and regulation in *Schizosaccharomyces pombe*. *Biochem. Soc. Trans.* **41,** 1679–1686
3. Halliwell, B., and Gutteridge, J. M. (1992) Biologically relevant metal ion-dependent hydroxyl radical generation. An update. *FEBS Lett.* **307,** 108–112
4. Labbé, S., Beaudoin, J., and Ioannoni, R. (2013) in *Metals in Cells* (Culotta, V. C., and Scott, R. S., eds) pp. 163–174, John Wiley & Sons, Chichester, UK
5. Zhou, H., and Thiele, D. J. (2001) Identification of a novel high affinity copper transport complex in the fission yeast *Schizosaccharomyces pombe*. *J. Biol. Chem.* **276,** 20529–20535
6. Beaudoin, J., Laliberté, J., and Labbé, S. (2006) Functional dissection of Ctr4 and Ctr5 amino-terminal regions reveals motifs with redundant roles in copper transport. *Microbiology* **152,** 209–222
7. Puig, S., Lee, J., Lau, M., and Thiele, D. J. (2002) Biochemical and genetic analyses of yeast and human high affinity copper transporters suggest a conserved mechanism for copper uptake. *J. Biol. Chem.* **277,** 26021–26030
8. Aller, S. G., Eng, E. T., De Feo, C. J., and Unger, V. M. (2004) Eukaryotic CTR copper uptake transporters require two faces of the third transmembrane domain for helix packing, oligomerization, and function. *J. Biol. Chem.* **279,** 53435–53441
9. Beaudoin, J., Thiele, D. J., Labbé, S., and Puig, S. (2011) Dissection of the relative contribution of the *Schizosaccharomyces pombe* Ctr4 and Ctr5 proteins to the copper transport and cell surface delivery functions. *Microbiology* **157,** 1021–1031
10. Ioannoni, R., Beaudoin, J., Mercier, A., and Labbé, S. (2010) Copper-dependent trafficking of the Ctr4-Ctr5 copper transporting complex. *PLoS ONE* **5,** e11964
11. Labbé, S., Peña, M. M., Fernandes, A. R., and Thiele, D. J. (1999) A copper-sensing transcription factor regulates iron uptake genes in *Schizosaccharomyces pombe*. *J. Biol. Chem.* **274,** 36252–36260
12. Peter, C., Laliberté, J., Beaudoin, J., and Labbé, S. (2008) Copper distributed by Atx1 is available to copper amine oxidase 1 in *Schizosaccharomyces pombe*. *Eukaryot. Cell.* **7,** 1781–1794
13. Bellemare, D. R., Shaner, L., Morano, K. A., Beaudoin, J., Langlois, R., and Labbe, S. (2002) Ctr6, a vacuolar membrane copper transporter in *Schizosaccharomyces pombe*. *J. Biol. Chem.* **277,** 46676–46686
14. Rees, E. M., Lee, J., and Thiele, D. J. (2004) Mobilization of intracellular copper stores by the Ctr2 vacuolar copper transporter. *J. Biol. Chem.* **279,** 54221–54229
15. Rees, E. M., and Thiele, D. J. (2007) Identification of a vacuole-associated metalloreductase and its role in Ctr2-mediated intracellular copper mobilization. *J. Biol. Chem.* **282,** 21629–21638
16. Marston, A. L., and Amon, A. (2004) Meiosis. Cell-cycle controls shuffle and deal. *Nat. Rev. Mol. Cell Biol.* **5,** 983–997
17. Handel, M. A., and Schimenti, J. C. (2010) Genetics of mammalian meiosis. Regulation, dynamics, and impact on fertility. *Nat. Rev. Genet.* **11,** 124–136
18. Kim, A. M., Vogt, S., O'Halloran, T. V., and Woodruff, T. K. (2010) Zinc availability regulates exit from meiosis in maturing mammalian oocytes. *Nat. Chem. Biol.* **6,** 674–681
19. Beaudoin, J., Ioannoni, R., López-Maury, L., Bähler, J., Ait-Mohand, S., Guérin, B., Dodani, S. C., Chang, C. J., and Labbé, S. (2011) Mfc1 is a novel forespore membrane copper transporter in meiotic and sporulating cells. *J. Biol. Chem.* **286,** 34356–34372
20. Bernhardt, M. L., Kong, B. Y., Kim, A. M., O'Halloran, T. V., and Woodruff, T. K. (2012) A zinc-dependent mechanism regulates meiotic progression in mammalian oocytes. *Biol. Reprod.* **86,** 114
21. Harigaya, Y., and Yamamoto, M. (2007) Molecular mechanisms underlying the mitosis-meiosis decision. *Chromosome Res.* **15,** 523–537
22. Bähler, J., Schuchert, P., Grimm, C., and Kohli, J. (1991) Synchronized meiosis and recombination in fission yeast. Observations with *pat1-114* diploid cells. *Curr. Genet.* **19,** 445–451
23. Doll, E., Molnar, M., Cuanoud, G., Octobre, G., Latypov, V., Ludin, K., and Kohli, J. (2008) Cohesin and recombination proteins influence the $G_1$-to-S transition in azygotic meiosis in *Schizosaccharomyces pombe*. *Genetics* **180,** 727–740
24. Mata, J., Lyne, R., Burns, G., and Bähler, J. (2002) The transcriptional program of meiosis and sporulation in fission yeast. *Nat. Genet.* **32,** 143–147
25. Mata, J., Wilbrey, A., and Bähler, J. (2007) Transcriptional regulatory network for sexual differentiation in fission yeast. *Genome Biol.* **8,** R217
26. Ioannoni, R., Beaudoin, J., Lopez-Maury, L., Codlin, S., Bahler, J., and Labbe, S. (2012) Cuf2 is a novel meiosis-specific regulatory factor of meiosis maturation. *PLoS ONE* **7,** e36338
27. Sabatinos, S. A., and Forsburg, S. L. (2010) Molecular genetics of *Schizosaccharomyces pombe*. *Methods Enzymol.* **470,** 759–795
28. Zhang, M. M., Wu, P. Y., Kelly, F. D., Nurse, P., and Hang, H. C. (2013) Quantitative control of protein S-palmitoylation regulates meiotic entry in fission yeast. *PLoS Biol.* **11,** e1001597
29. Keeney, J. B., and Boeke, J. D. (1994) Efficient targeted integration at *leu1-32* and *ura4-294* in *Schizosaccharomyces pombe*. *Genetics* **136,** 849–856
30. Nevitt, T., and Thiele, D. J. (2011) Host iron withholding demands siderophore utilization for *Candida glabrata* to survive macrophage killing. *PLoS Pathog.* **7,** e1001322
31. Chen, D., Toone, W. M., Mata, J., Lyne, R., Burns, G., Kivinen, K., Brazma, A., Jones, N., and Bähler, J. (2003) Global transcriptional responses of fission yeast to environmental stress. *Mol. Biol. Cell* **14,** 214–229
32. Mercier, A., Watt, S., Bähler, J., and Labbé, S. (2008) Key function for the CCAAT-binding factor Php4 to regulate gene expression in response to iron deficiency in fission yeast. *Eukaryot. Cell.* **7,** 493–508
33. Beaudoin, J., and Labbé, S. (2001) The fission yeast copper-sensing transcription factor Cuf1 regulates the copper transporter gene expression through an Ace1/Amt1-like recognition sequence. *J. Biol. Chem.* **276,** 15472–15480
34. Mercier, A., Pelletier, B., and Labbé, S. (2006) A transcription factor cascade involving Fep1 and the CCAAT-binding factor Php4 regulates gene expression in response to iron deficiency in the fission yeast *Schizosaccharomyces pombe*. *Eukaryot. Cell* **5,** 1866–1881
35. Pouliot, B., Jbel, M., Mercier, A., and Labbé, S. (2010) *abc3*$^+$ encodes an iron-regulated vacuolar ABC-type transporter in *Schizosaccharomyces pombe*. *Eukaryot. Cell* **9,** 59–73
36. Laliberté, J., Whitson, L. J., Beaudoin, J., Holloway, S. P., Hart, P. J., and Labbé, S. (2004) The *Schizosaccharomyces pombe* Pccs protein functions in both copper trafficking and metal detoxification pathways. *J. Biol. Chem.* **279,** 28744–28755
37. Li, L., Chen, O. S., McVey Ward, D., and Kaplan, J. (2001) CCC1 is a transporter that mediates vacuolar iron storage in yeast. *J. Biol. Chem.* **276,** 29515–29519
38. MacDiarmid, C. W., Milanick, M. A., and Eide, D. J. (2002) Biochemical properties of vacuolar zinc transport systems of *Saccharomyces cerevisiae*. *J. Biol. Chem.* **277,** 39187–39194
39. MacDiarmid, C. W., Gaither, L. A., and Eide, D. (2000) Zinc transporters that regulate vacuolar zinc storage in *Saccharomyces cerevisiae*. *EMBO J.* **19,** 2845–2855
40. Abe, H., and Shimoda, C. (2000) Autoregulated expression of *Schizosaccharomyces pombe* meiosis-specific transcription factor Mei4 and a genome-wide search for its target genes. *Genetics.* **154,** 1497–1508
41. Nakamura, T., Nakamura-Kubo, M., Hirata, A., and Shimoda, C. (2001) The *Schizosaccharomyces pombe spo3*$^+$ gene is required for assembly of the forespore membrane and genetically interacts with psy1(+)-encoding syntaxin-like protein. *Mol. Biol. Cell* **12,** 3955–3972
42. Nakamura, T., Asakawa, H., Nakase, Y., Kashiwazaki, J., Hiraoka, Y., and Shimoda, C. (2008) Live observation of forespore membrane formation in

fission yeast. *Mol. Biol. Cell* **19,** 3544–3553
43. Miller, E. W., Zeng, L., Domaille, D. W., and Chang, C. J. (2006) Preparation and use of Coppersensor-1, a synthetic fluorophore for live-cell copper imaging. *Nat. Protoc.* **1,** 824–827
44. Zeng, L., Miller, E. W., Pralle, A., Isacoff, E. Y., and Chang, C. J. (2006) A selective turn-on fluorescent sensor for imaging copper in living cells. *J. Am. Chem. Soc.* **128,** 10–11
45. Liu, X. F., Elashvili, I., Gralla, E. B., Valentine, J. S., Lapinskas, P., and Culotta, V. C. (1992) Yeast lacking superoxide dismutase. Isolation of genetic suppressors. *J. Biol. Chem.* **267,** 18298–18302
46. Nakase, Y., Nakamura, T., Hirata, A., Routt, S. M., Skinner, H. B., Bankaitis, V. A., and Shimoda, C. (2001) The *Schizosaccharomyces pombe spo20*$^+$ gene encoding a homologue of *Saccharomyces cerevisiae* Sec14 plays an important role in forespore membrane formation. *Mol. Biol. Cell* **12,** 901–917
47. Nakamura-Kubo, M., Nakamura, T., Hirata, A., and Shimoda, C. (2003) The fission yeast *spo14*$^+$ gene encoding a functional homologue of budding yeast Sec12 is required for the development of forespore membranes. *Mol. Biol. Cell* **14,** 1109–1124
48. Nakamura, T., Kashiwazaki, J., and Shimoda, C. (2005) A fission yeast SNAP-25 homologue, SpSec9, is essential for cytokinesis and sporulation. *Cell Struct. Funct.* **30,** 15–24
49. Takegawa, K., Iwaki, T., Fujita, Y., Morita, T., Hosomi, A., and Tanaka, N. (2003) Vesicle-mediated protein transport pathways to the vacuole in *Schizosaccharomyces pombe*. *Cell Struct. Funct.* **28,** 399–417
50. Ohtaka, A., Okuzaki, D., and Nojima, H. (2008) Mug27 is a meiosis-specific protein kinase that functions in fission yeast meiosis II and sporulation. *J. Cell Sci.* **121,** 1547–1558